SPECIAL TOPIC — Advanced calculation & characterization of energy storage materials & devices at multiple scale

Revealing the inhomogeneous surface chemistry on the spherical layered oxide polycrystalline cathode particles*

Zhi-Sen Jiang(蒋之森)[1], Shao-Feng Li(李少锋)[2], Zheng-Rui Xu(许正瑞)[3], Dennis Nordlund[2], Hendrik Ohldag[2], Piero Pianetta[2], Jun-Sik Lee[2,†], Feng Lin(林锋)[3,‡], and Yi-Jin Liu(刘宜晋)[2,§]

[1] *College of Physics, Sichuan University, Chengdu* 610065, *China*
[2] *Stanford Synchrotron Radiation Lightsource, SLAC National Accelerator Laboratory, Menlo Park, CA* 94025, *USA*
[3] *Department of Chemistry, Virginia Tech, Blacksburg, VA* 24061, *USA*

(Received 16 November 2019; revised manuscript received 20 December 2019; accepted manuscript online 25 December 2019)

The hierarchical structure of the composite cathodes brings in significant chemical complexity related to the interfaces, such as cathode electrolyte interphase. These interfaces account for only a small fraction of the volume and mass, they could, however, have profound impacts on the cell-level electrochemistry. As the investigation of these interfaces becomes a crucial topic in the battery research, there is a need to properly study the surface chemistry, particularly to eliminate the biased, incomplete characterization provided by techniques that assume the homogeneous surface chemistry. Herein, we utilize nano-resolution spatially-resolved x-ray spectroscopic tools to probe the heterogeneity of the surface chemistry on $LiNi_{0.8}Mn_{0.1}Co_{0.1}O_2$ layered cathode secondary particles. Informed by the nano-resolution mapping of the Ni valance state, which serves as a measurement of the local surface chemistry, we construct a conceptual model to elucidate the electrochemical consequence of the inhomogeneous local impedance over the particle surface. Going beyond the implication in battery science, our work highlights a balance between the high-resolution probing the local chemistry and the statistical representativeness, which is particularly vital in the study of the highly complex material systems.

Keywords: Ni-rich cathode, x-ray nanoprobe, redox heterogeneity, surface chemistry

PACS: 61.05.cj, 78.70.Dm, 87.59.–e, 82.45.Fk **DOI:** 10.1088/1674-1056/ab6585

1. Introduction

Layered transition metal oxides, e.g., $LiNi_xMn_yCo_zO_2$ (NMC), are state-of-the-art industry-relevant battery cathode materials.[1] They are often in the form of secondary particles at 5–20 μm in diameter and are embedded in porous carbon-binder matrix forming hierarchically structured composite electrodes.[2] The layered lattice structure offers two-dimensional lithium diffusion pathways. It hosts and releases the lithium-ions at the discharged and the charged states, respectively. Undesired phase transformations, however, could occur in the cathode and could be provoked by the elevated temperature,[3] deep delithiation,[4] oxygen release,[5] and cathode electrolyte interphase formation.[6–8] It is well-known that such unwanted phase transformations, for example, from layered structure to spinel and/or rocksalt structures, would negatively impact the cell performance as they preferably take place over the particle surface and, thus, could increase the impedance by passivating the NMC particle surface.[9] Similar surface degradation takes place universally in oxide cathodes for sodium ion batteries.[10] While this is a common degradation mechanism and is generally applicable, we would point out that the spatial heterogeneity of the surface phase transformation is ubiquitous and impactful, and yet, is often overlooked. Several groups have emphasized the importance of applying characterization techniques that are sensitive to multiple length scales to investigate these heterogenous behaviors.[11,12] Lin *et al.* combined ensemble-averaged x-ray spectroscopy and spatially resolved electron microscopy to show that the surface degradation is heterogeneous in NMC particles. It is heterogeneous not only along different crystal directions of an NMC particle but also between different NMC particles.[13] This heterogenous phenomenon has not been considered in a large body of the published literature. Our recent study has taken the particle-to-particle heterogeneity into account, and investigated hundreds of secondary NMC particles to yield a scientific interpretation with statistical significance.[2] In the present study, we investigate the inhomogeneous surface chemistry on an isotropic, single layered oxide polycrystalline cathode particle.

The inhomogeneity in the surface degradation at the particle level could have more complicated consequence than the simple expression of "surface passivation". The regions that undergo significant surface degradation may build up an impedance layer that impedes the Li ion transport thus under-

*Project supported by U.S. Department of Energy, Office of Science, Office of Basic Energy Sciences under Contract No. DE-AC02-76SF00515 and National Science Foundation under Grant No. DMR-1832613.
†Corresponding author. E-mail: jslee@slac.stanford.edu
‡Corresponding author. E-mail: fenglin@vt.edu
§Corresponding author. E-mail: liuyijin@slac.stanford.edu

mining the contribution of the particles to the capacity. On the other hand, the surface degradation may be taken advantage of to improve the long term stability of the cathode particles. For example, Mu *et al.* used side reactions between electrolyte solvents and layered oxide particles to create a passivation layer on the particle surface, which lowered the initial capacity but provided an improved cycling stability upon extensive cycling.[14] This is because the pre-passivation prior to the electrochemistry can offers a protection mechanism to mitigate the cathode-electrolyte side reactions during the electrochemical cycling. Therefore, more efforts are needed to understand the impact of surface degradation, and the first step is to properly characterize the surface chemistry with a balance between the high-resolution probing the local chemistry and the statistical representativeness.

Experimental evidence on the inhomogeneous surface chemistry is not yet convincingly demonstrated for polycrystalline secondary particles. Reports available in the literature largely rely on very localized experimental probes for primary particles, which could raise questions regarding the representativeness of the observation. Nano-resolution chemical mapping over representative secondary particles of the NMC cathode is yet to be demonstrated and constitutes a frontier challenge in this field. Herein, we utilize a suite of cutting-edge synchrotron techniques, including the soft x-ray absorption spectroscopy (soft XAS), soft x-ray nanoprobe, and hard x-ray nano-resolution spectro-tomography[15] to tackle the question regarding the inhomogeneity of the surface chemistry in a systematic manner. We illustrate that the redox heterogeneity is unambiguously present over the surface of the NMC secondary particle, which lays out the basis for a conceptual model to describe the potential impact of the inhomogeneous surface degradation on the electrochemical performance of individual secondary particles.

2. Experiments

2.1. Electrode preparation, electrochemistry, and sample preparation

The NMC811 cathode powder was provided by the U.S. Department of Energy's (DOE) Cell Analysis, Modeling and Prototyping (CAMP) Facility, Argonne National Laboratory. The cathode slurry was prepared by mixing 90 wt.% active material, 5 wt.% polyvinylidene fluoride, and 5 wt.% acetylene carbon black in N-methyl-2-pyrrolidone. After that, the slurry was cast onto a carbon-coated aluminum foil current collector, forming a cathode sheet. This cathode sheet was vacuum dried at 120 ℃ for 12 h. The lithium metal anode, glass fiber separator, and thin film cathode were assembled into a CR2032-type coin cell in an argon-filled glovebox. 1 M $LiPF_6$ dissolved in a 3 : 7 weight ratio of ethylene carbonate/ethyl methyl carbonate with 2 wt.% vinylene carbonate was used as the electrolyte. All the electrochemical testing was conducted using a Neware battery testing system. 1 C was defined as fully charging the cathode in 1 h, with a specific capacity of 200 mA·h/g.

2.2. Soft x-ray absorption spectroscopy in TEY mode

Soft x-ray nanoprobe was conducted at beamline 13-1 of the Stanford Synchrotron Radiation Lightsource (SSRL) of the SLAC National Accelerator Laboratory. This soft x-ray nanoprobe setup is housed in a vacuum chamber, which is typically operated at a pressure of 2×10^{-8} mbar. A Fresnel zone plate is used to focus the x-ray beam to a spot of about 30 nm. The distance between the zone plate and the pinhole is adjusted as a function of x-ray energy due to the change in the focal length. Soft x-ray nanoprobe mapping is conducted by raster scanning the sample in the focal plane of the beam. The total electron yield (TEY) signal is acquired by point-to point scanning at 852.0 eV and 854.2 eV, respectively. The data analysis was performed using TXM-Wizard,[16] an in-house-developed software package.

2.3. Soft x-ray nanoprobe at beamline 13-3 of SSRL

Soft XAS measurements were carried out at the elliptically polarizing undulator (EPU) beamline 13-3 at SSRL. The NMC811 electrode was recovered from a conventional coin cell with liquid electrolyte. After being disassembled, the electrode was dried in an ultra-high vacuum environment before the soft x-ray measurements. The LMR electrodes were mounted using the conductive carbon tape onto a sample holder for measurement in an ultra-high vacuum (UHV) chamber. The vertically polarized x-ray (sigma-polarization) was used. The incident beam was monochromatized using a 600-lines/mm spherical grating monochromator (SGM), and its angle was set at 30° from the sample surface. All the XAS spectra were normalized by the intensity of the incoming x-ray beam that was concurrently measured by monitoring the drain current on an electrically isolated gold-coated mesh. A linear background was subtracted from the data before further interpretation.

2.4. Hard x-ray nano-resolution spectro-tomography at beamline 6-2 of SSRL

The x-ray spectro-microscopic scans of deeply charged $Li_{0.5}Ni_{0.8}Mn_{0.1}Co_{0.1}O_2$ (NMC811) particles were carried out using the transmission x-ray microscopy (TXM) at beamline 6-2C of SSRL of the SLAC National Accelerator Laboratory. The NMC811 particles were loaded into a quartz capillary (100 μm in diameter and 10 μm in wall thickness). The typical exposure time for single images was 0.5 s. The nominal spatial resolution of this instrument is $\sim$ 30 nm. More details of the synchrotron beamline configuration and the concept of x-ray spectro-microscopy and spectro-tomography can be found elsewhere.[15] In the 3D XANES scan, tomography was per-

formed at 74 different energy levels across the XANES energy window (8203–8575 eV). In the near edge region (8324–8376 eV), we chose the energy step at 1 eV; the pre-edge and post-edge regions were scanned with larger energy steps of 5 eV, 10 eV, and 20 eV for covering a wide energy window to execute the normalization of the spectra. The TXM data reduction was conducted using TXM-Wizard.[16]

3. Result and discussion

3.1. Soft XAS signal averaged over the large footprint of x-ray illumination

Soft x-ray absorption spectroscopy has been broadly utilized to characterize the chemical state over the surface of the composite electrode. In particular, due to the difference in their probing depths, the detections of electron and fluorescence yields (TEY and FY) as a function of the excitation energy have been used to reveal the chemical fingerprints over the top-5-nm surface and the up-to-100-nm subsurface regions,[17] respectively. In the current study, the TEY signal is presented because the surface chemistry is our focus. We point out that, in this section, the detected signal is averaged over a large footprint of the x-ray illumination, which is at millimeter scale in the current experiment. As shown in Fig. 1(a), the valence state of Ni can nicely benchmark the different phases that are present in degraded NMC particles (Fig. 1(b)). Upon charging, the Li ions are extracted from the layered structure, taking an electron (per Li-ion) from the transition metal cations (assuming no oxygen redox) for keeping the entire cathode charge neutral (Figs. 1(c) and 1(d)). At the fully charged state, the Ni cation in the layered NMC lattice exhibits a high valence state between Ni^{3+} and Ni^{4+} and the peak at excitation energy of 856.2 eV is significantly stronger than the peak at 854 eV (blue curve in Fig. 1(a)). The layered NMC structure, however, tends to collapse at deeply charged state, forming a rock-salt structure at the surface (Fig. 1(e)), which does not offer proper Li diffusion pathways. The Ni cation in the rock-salt phase exhibits a valence state of Ni^{2+}, whose soft XAS fingerprint is plotted in Fig. 1(a) (orange curve). The TEY data acquired from our charged NMC sample is the red curve in Fig. 1(a), which appears to be similar to that of the rock-salt phase, however the peak at 856.2 eV is more enhanced, indicating that the cathode surface is not fully reduced to Ni^{2+} that correlates with the rock-salt structures. Therefore, our data suggests an incomplete surface transformation (either chemically or spatially), posing an interesting question that urges for a comprehensive investigation using experimental tools with sufficient spatial resolution as well as the chemical sensitivity.

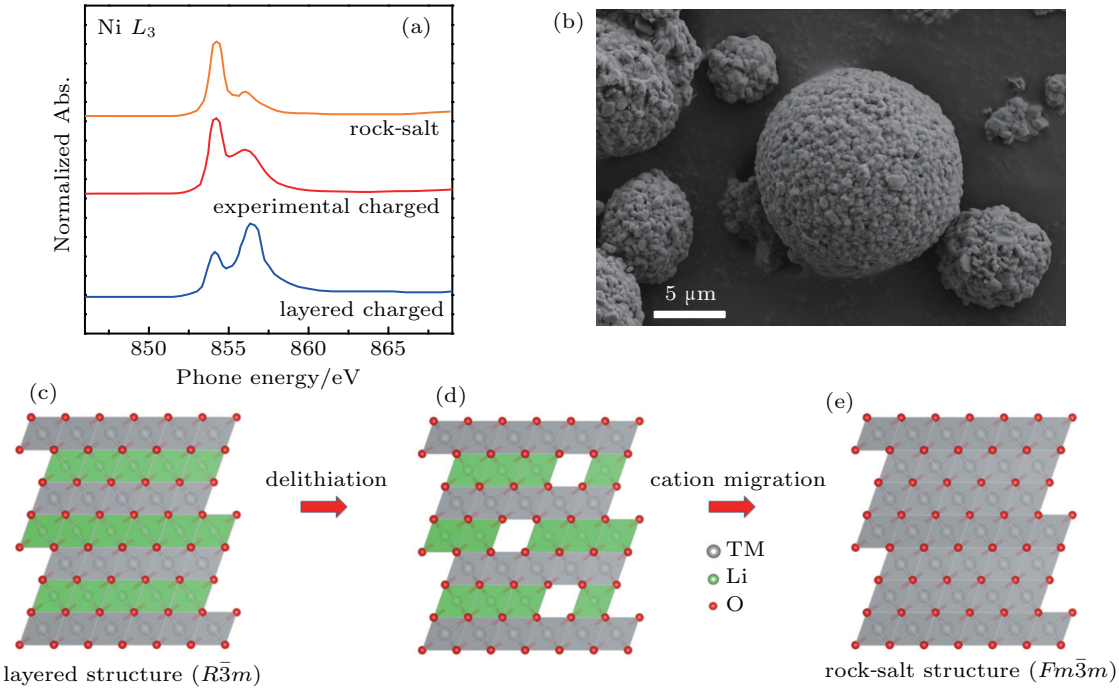

Fig. 1. (a) The spectroscopic fingerprints of the $LiNi_{0.8}Mn_{0.1}Co_{0.1}O_2$ cathode over the Ni L_3-edge at different states. (b) SEM image of typical NMC811 secondary particles. (c)–(e) Illustration of the phase transformation in the NMC lattice upon charging. The transformation to the rocksalt phase usually takes place at the surface region of the NMC particles.

3.2. Heterogeneous surface chemistry revealed by soft x-ray nanoprobe

As discussed above, the TEY signal averaged over a large beam footprint does not offer a comprehensive understanding of the incomplete surface transformation. Therefore, we employed the soft x-ray nanoprobe (available at beamline 13-1 of SSRL, see Fig. 2(a) for the schematic) to complement the data in the previous section. A FZP is used to focus the incoming x-rays to a 30 nm spot, which is used to raster scan

the sample to collect the spatially resolved TEY signal. As illustrated in Fig. 2(b), the theoretically calculated spectra of phase-pure Ni^{2+} and Ni^{3+} (solid line) exhibit distinguished peak positions. Therefore, the intensity ratio between these two peaks can be used to quantify the relative Ni valence state. The difference between the two dashed lines in Fig. 2(b) suggests that different locations on the electrode could have different Ni valence states. Based on this, we choose to conduct the TEY mapping of an arbitrarily selected particle from the composite electrode using 854 eV and 856.2 eV, respectively (see Fig. 2(c)). The ratio of the 856.2 eV scan to the sum of the scans at 854 eV and 856.2 eV is calculated to elucidate the relative Ni valence state over the scanned particle surface. The calculated ratio map is color coded with the red and blue indicating higher and lower Ni valence, respectively. Color heterogeneity is clearly observed in the map shown in the right panel of Fig. 2(c), highlighting the variation in the localized surface chemistry.

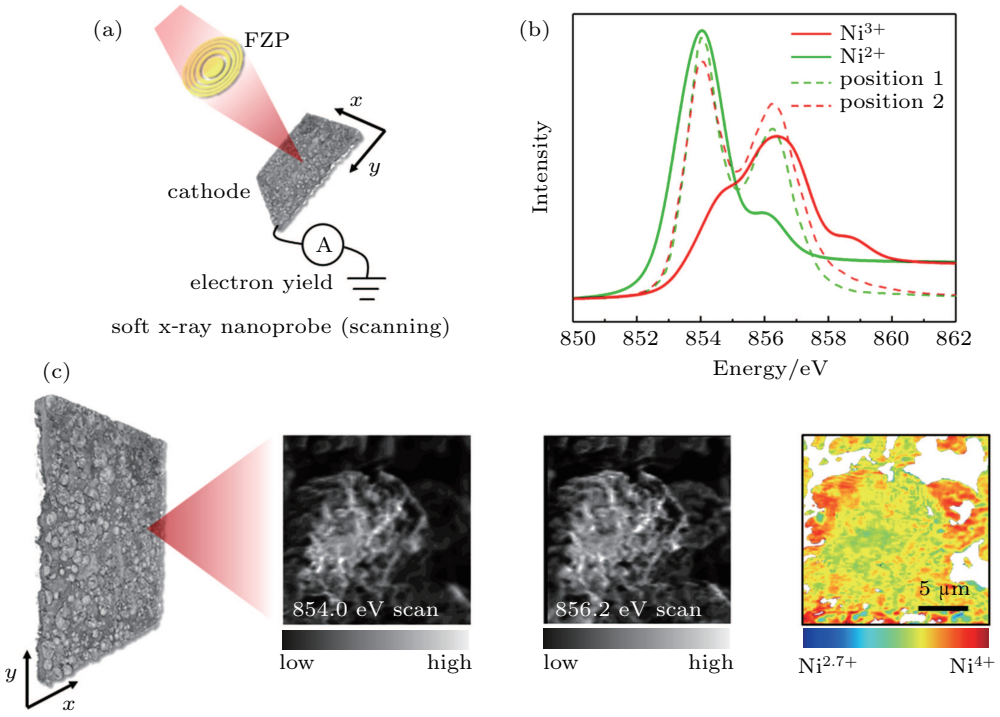

Fig. 2. Heterogeneity in the Ni valence state distribution over the surface of an individual NMC particle. Panel (a) illustrates the schematic of the soft x-ray nanoprobe for mapping the TEY signal with a 30 nm focal spot. Panel (b) shows spectroscopic signature of phase-pure Ni^{2+} and Ni^{3+} (solid line) as well as that of different regions on the particle surface (dashed lines). Panel (c) illustrates our approach to reveal the relative Ni valence states over the imaged particle surface. The scale bar in panel (c) is 5 μm.

3.3. Heterogeneous redox state over the particle surface revealed by nano-resolution hard x-ray spectro-tomography

The soft x-ray nanoprobe offers excellent sensitivity to the local surface chemistry. It, however, can only probe the exposed surface of the particle. In the composite electrode, majority of the particles are buried in the porous carbon binder matrix, which makes them inaccessible by the soft x-ray probes. To tackle this issue, we isolated a single NMC particle and used hard x-ray spectro-tomography to investigate this particle in its entirety. The concept of the full-field spectro-microscopy technique is illustrated in Figs. 3(a) and 3(b). Full-field transmission images of the sample are acquired as the incoming energy is tuned across the absorption edge of Ni. After a number of image processing steps,[15] a hard x-ray absorption spectrum can be extracted for every single spatial unit (i.e., a pixel), allowing for the quantification of the local Ni valence state via detecting the edge energy (Fig. 3(b)). This procedure is repeated pixel by pixel, and the 2D projective imaging is conducted at different angles to facilitate the reconstruction of the 3D Ni valence distribution (Fig. 3(c)). Because we are focusing on the surface chemistry, we carry out a cylindrical map projection (similar to the 2D world map of the 3D Earth) and demonstrate the valence map over the entire particle surface in Fig. 3(d). In addition to the Ni valence state inhomogeneity over the particle surface, it is interesting to note that the deeply charged regions (red) and the deeply reduced regions (blue) both appear to be isolated domains. This observation further highlights the fact that the charge heterogeneity and the surface degradation can be highly dependent on the location of a relatively isotropic NMC secondary particle. Therefore, we point out here that the investigation of the surface degradation using ultrahigh resolution probes (e.g., TEM) shall be carried out cautiously to have statistical representativeness.

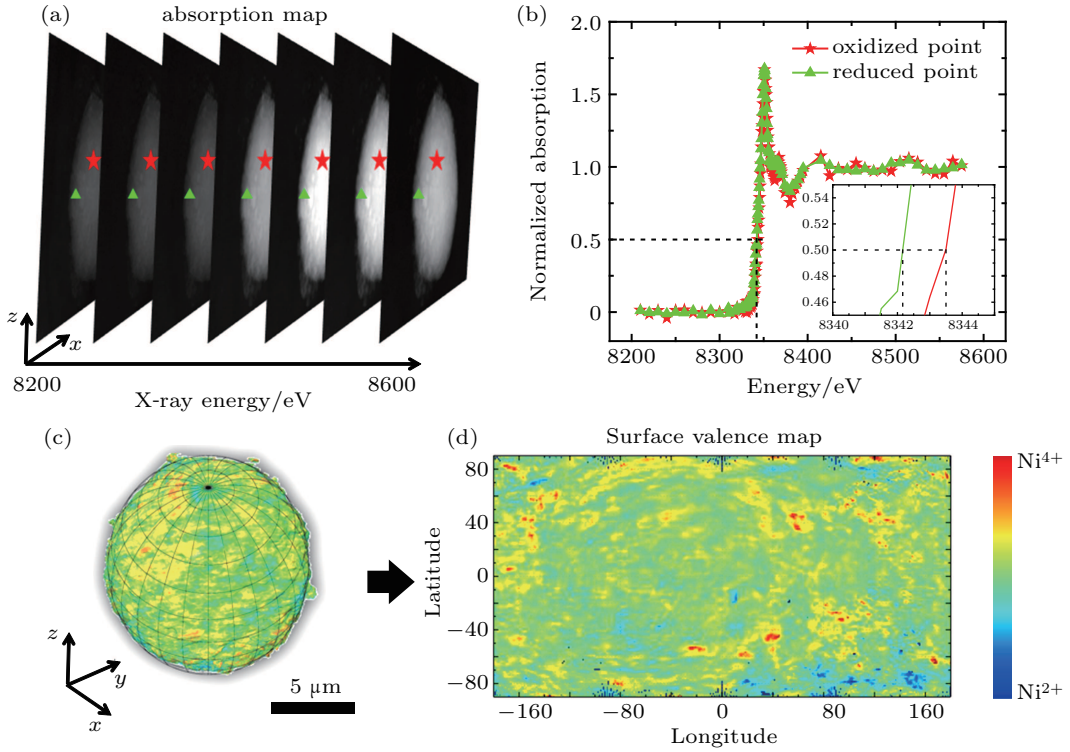

Fig. 3. Hard x-ray spectro-microscopic study of the Ni valence state heterogeneity in an NMC particle. Panels (a) and (b) illustrate the concept of the full-field hard x-ray spectro-microscopy. Panel (c) shows the reconstructed 3D Ni valence distribution over the scanned NMC particle. Panel (d) shows the cylindrically projected particle surface for a better visualization of the entire particle surface. The scale bar in panel (c) is 5 μm.

3.4. A conceptual model to understand the impact of inhomogeneous surface chemistry on the electrochemical behavior of an NMC particle

With input from both soft x-ray nanoprobe and hard x-ray nano-resolution spectro-tomography, we confirmed that the surface chemistry is highly inhomogeneous over the NMC particle surface. The regions with a higher state of charge would have a high degree of side reactions with the electrolyte, leading to the inhomogeneous surface degradation over the particle surface. Such phenomenon could have a profound impact on the particle's electrochemical behavior. Here we propose a simple conceptual model to elucidate such effect. As show in Fig. 4(a), in an ideal spherical particle, the diffusion of Li goes from the center toward the surface upon charging (white arrows). Generally speaking, the center of the particle has longer diffusion length due to the geometrical constrain and, therefore, the effective local impedance is concentric rings. The partial surface degradation, however, breaks the symmetry. As illustrated in Fig. 4(b), the lower left of the particle is more significantly impacted by the surface passivation (the red arc in Fig. 4(b)). The regions within the particle would be significantly affected because the diffusion of Li could go through geometrically longer path with smaller resistance or geometrically shorter path with larger resistance. Depending on the degree of surface degradation and, more importantly, its spatial arrangement, the kinetically favored diffusion pathways could be dramatically altered, and the mesoscale charge and redox heterogeneity can be rearranged. While our current conceptual model has simplified microstructural complexity of the polycrystalline NMC particles, we anticipate that our experimental results can motivate more studies in the field to consider the inhomogeneous nature of the surface chemistry and degradation.

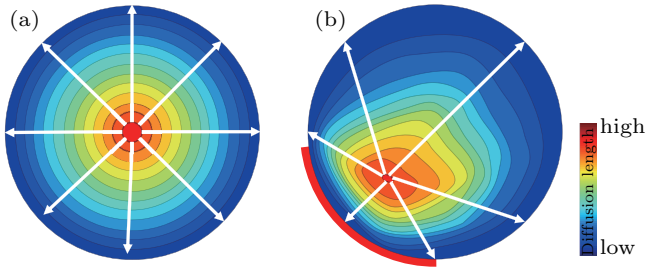

Fig. 4. Schematic illustration of the partial surface passivation induced rearrangement of the kinetically favored Li diffusion pathways in NMC cathode particle. Panel (a) shows the ideal case with no surface degradation. Panel (b) shows how the particle is affected by the passivation of part of the particle surface (the red arc).

4. Conclusion

Properly characterizing the surface chemistry of battery particles can provide experimental inputs to understand the complex interplay between the electrode and the electrolyte. It has remained a key challenge to perform the characterization with both the high-resolution probing the local chemistry and the statistical representativeness. In this study, we demonstrate the capability of characterizing the inhomogeneous surface chemistry with advanced synchrotron spectro-

scopic probes. The surface of $LiNi_{0.8}Mn_{0.1}Co_{0.1}O_2$ particles exhibits a high degree of inhomogeneous state of charge distribution. We understand that the similar level of characterization is still quite challenging without the combination of synchrotron spectroscopic imaging methods, and that these advanced characterization methods are not readily available to many research groups. We believe that the lab scale characterization, such as electron microscopy, can still have a balance between the high-resolution probing the local chemistry and the statistical representativeness if many particles are studied, not deducing conclusions based on only a limited number of particles.

Acknowledgments

Use of the Stanford Synchrotron Radiation Lightsource, SLAC National Accelerator Laboratory is supported by the U.S. Department of Energy, Office of Science, Office of Basic Energy Sciences under Contract No. DE-AC02-76SF00515. F. L. acknowledges the support from the National Science Foundation under Grant No. DMR-1832613. The engineering support from D. Van Campen, D. Day, and V. Borzenets for the TXM experiment at beamline 6-2C of SSRL is gratefully acknowledged.

References

[1] Xu J, Lin F, Doeff M M and Tong W 2017 *J. Mater. Chem. A* **5** 874

[2] Yang Y, Xu R, Zhang K, Lee S, Mu L, Liu P, Waters C K, Spence S, Xu Z, Wei C, Kautz D J, Yuan Q, Dong Y, Yu Y, Xiao X, Lee H, Pianetta P, Cloetens P, Lee J, Zhao K, Lin F and Liu Y 2019 *Adv. Energy Mater.* **9** 1900674

[3] Wei C, Zhang Y, Lee S J, Mu L, Liu J, Wang C, Yang Y, Doeff M, Pianetta P, Nordlund D, Du X W, Tian Y, Zhao K, Lee J S, Lin F and Liu Y 2018 *J. Mater. Chem. A* **6** 23055

[4] Mao Y, Wang X, Xia S, Zhang K, Wei C, Bak S, Shadike Z, Liu X, Yang Y, Xu R, Pianetta P, Ermon S, Stavitski E, Zhao K, Xu Z, Lin F, Yang X, Hu E and Liu Y 2019 *Adv. Funct. Mater.* **29** 1900247

[5] Mu L, Lin R, Xu R, Han L, Xia S, Sokaras D, Steiner J D, Weng T C, Nordlund D, Doeff M M, Liu Y, Zhao K, Xin H L and Lin F 2018 *Nano Lett.* **18** 3241

[6] Lin F, Nordlund D, Li Y, Quan M K, Cheng L, Weng T C, Liu Y, Xin H L and Doeff M M 2016 *Nat. Energy* **1** 15004

[7] Yan P, Nie A, Zheng J, Zhou Y, Lu D, Zhang X, Xu R, Belharouak I, Zu X, Xiao J, Amine K, Liu J, Gao F, Shahbazian-Yassar R, Zhang J G and Wang C M 2015 *Nano Lett.* **15** 514

[8] Jung S K, Gwon H, Hong J, Park K Y, Seo D H, Kim H, Hyun J, Yang W and Kang K 2014 *Adv. Energy Mater.* **4** 1300787

[9] Lin F, Markus I M, Nordlund D, Weng T C, Asta M D, Xin H L and Doeff M M 2014 *Nat. Commun.* **5** 3529

[10] Mu L, Feng X, Kou R, Zhang Y, Guo H, Tian C, Sun C J, Du X W, Nordlund D, Xin H L and Lin F 2018 *Adv. Energy Mater.* **8** 1801975

[11] Wolf M, May B M and Cabana J 2017 *Chem. Mater.* **29** 3347

[12] Lin F, Liu Y, Yu X, Cheng L, Singer A, Shpyrko O G, Xin H L, Tamura N, Tian C, Weng T C, Yang X Q, Meng Y S, Nordlund D, Yang W and Doeff M M 2017 *Chem. Rev.* **117** 13123

[13] Lin F, Markus I M, Nordlund D, Weng T C, Asta M D, Xin H L and Doeff M M 2014 *Nat. Commun.* **5** 3529

[14] Mu L, Rahman M M, Zhang Y, Feng X, Du X W, Nordlund D and Lin F 2018 *J. Mater. Chem. A* **6** 2758

[15] Meirer F, Cabana J, Liu Y, Mehta A, Andrews J C and Pianetta P 2011 *J. Synchrotron Radiat.* **18** 773

[16] Liu Y, Meirer F, Williams P A, Wang J, Andrews J C and Pianetta P 2012 *J. Synchrotron Radiat.* **19** 281

[17] Tian C, Nordlund D, Xin H L, Xu Y, Liu Y, Sokaras D, Lin F and Doeff M M 2018 *J. Electrochem. Soc.* **165** A696